

Geochemical characteristics and geological genesis of soil selenium anomaly zone in the Hetao Plain, Inner Mongolia, and crop biological effects-based assessment of selenium-rich cultivated land development potential

Yong-chun Li, Guo-dong Chen, Yu-chun-zi Du, Jiu-fen Liu, Xue-zhen Li, Hong-bing Hou

Citation: Yong-chun Li, Guo-dong Chen, Yu-chun-zi Du, Jiu-fen Liu, Xue-zhen Li, Hong-bing Hou, 2026. Geochemical characteristics and geological genesis of soil selenium anomaly zone in the Hetao Plain, Inner Mongolia, and crop biological effects-based assessment of selenium-rich cultivated land development potential, China Geology, 9, 303-315. doi: 10.31035/cg2024037.

View online: https://doi.org/10.31035/cg2024037

Related articles that may interest you

Effects and mechanism of igneous rock on selenium in the tropical soil-rice system in Hainan Province, South China

China Geology. 2022, 5(1), 1 https://doi.org/10.31035/cg2021038

Characteristics of B, Zn and Se in stream sediments of Tanzania and their agricultural applications: Based on 1∶1000000 geochemical survey

China Geology. 2023, 6(1), 1 https://doi.org/10.31035/cg2022049

Conversion relationship of rainfall-soil moisture-groundwater in Quaternary thick cohesive soil in Jianghan Plain, Hubei Province, China

China Geology. 2020, 3(3), 462 https://doi.org/10.31035/cg2020053

Relationship between spatio-temporal evolution of soil pH and geological environment/surface cover in the eastern Nenjiang River Basin of Northeast China during the past 30 years

China Geology. 2023, 6(3), 369 https://doi.org/10.31035/cg2022062

Distribution characteristics, exploration and development, geological theories research progress and exploration directions of shale gas in China

China Geology. 2022, 5(1), 110 https://doi.org/10.31035/cg2021069

Distribution of potential geological hazards and control factors in Qingdao offshore, China

China Geology. 2019, 2(1), 40 https://doi.org/10.31035/cg2018074

China Geology 9 (2026) 303−315

China Geology

Journal homepage: http://chinageology.cgs.cn
https://www.sciencedirect.com/journal/china-geology



Geochemical characteristics and geological genesis of soil selenium anomaly zone in the Hetao Plain, Inner Mongolia, and crop biological effects-based assessment of selenium-rich cultivated land development potential

Yong-chun Li[a, b], Guo-dong Chen[a, b], Yu-chun-zi Du[a, b], Jiu-fen Liu[c, d, e], Xue-zhen Li[c], Hong-bing Hou[a, b,*]

[a] *Hohhot General Survey of Natural Resources Center, China Geological Survey, Ministry of Natural Resources, Hohhot* 010010, *China*
[b] *Innovation Base for Water Resource Exploration and Eco-environmental Effects in the Daheihe Basin of the Yellow River, Hohhot* 010010, *China*
[c] *School of Earth Sciences and Resources, China University of Geosciences (Beijing), Beijing* 100083, *China*
[d] *Natural Resources Comprehensive Survey Command Center, China Geological Survey, Beijing* 100055, *China*
[e] *Key Laboratory of Coupling Process and Effect of Natural Resources Elements, Beijing* 100055, *China*

ARTICLE INFO

Article history:
Received 11 March 2024
Received in revised form 11 October 2024
Accepted 1 November 2024
Available online 22 November 2024

Keywords:
Selenium
Soil parent material
Geological genesis
Channel sedimentary type
Selenium-rich cultivated land
Selenium-rich corn
Selenium-rich sunflower
Selenium-rich zucchini
Development and utilization potential
Hetao Plain
Yellow River ancient channel
Geological survey engineering

ABSTRACT

Exploring the geological genesis of selenium (Se) in Se-rich soil of the Hetao Plain, a major grain production base of corn, wheat, potato, sunflower and zucchini in northern China, is vital for the rational development of Se-rich land resources and the environmental geochemical assessment. In this study, element geochemical characterization, geospatial analysis and mathematical statistics were employed to investigate the factors influencing the spatial distribution of soil Se in the Hetao Plain, focusing on the differences in soil chemical weathering intensity, rare earth elements distribution pattern and soil sedimentary sequence characteristics between the study area and typical surrounding parent materials. The results indicated that the soil Se content in the study area ranged from 0.07 mg/kg to 0.72 mg/kg, with an average value of 0.24 mg/kg, which was higher than the regional background values. Moreover, this suggested that local Se enrichment occurred in the soil of study area, and that the Se distribution was restricted by factors including soil clay minerals, constant elements and soil organic matter (SOM) contents. The characteristics of soil parent material in the study area differed significantly from those of the piedmont diluvial parent material, whereas were similar to those of the Yellow River floodplain and lacustrine parent materials, revealing that the soil parent material in the study area mainly came from the water system transportation. Through combining the characteristics of soil sedimentary sequences in the study area with the location of the Yellow River ancient channel, it is suggested that the origin of high Se soil in the central and northern belt zone of the study area is associated with the Yellow River ancient channel, where the enrichment pattern is “channel sedimentary type”. In addition, the development and utilization potential of Se-rich cultivated land was explored based on the biological effects of Se. It was concluded that the Se content of crops (corn, sunflower and zucchini) in the study area was higher than that of similar crops in China, that crop species and soil Se content were the dominant influencing factors of crop Se content in the study area, and that the crops growing in Se-rich areas had higher Se enrichment rate than those growing in non-Se-rich areas. This exhibited a high development and utilization potential of the investigated cultivated land for Se-rich crop production.

©2026 China Geology Editorial Office.

1. Introduction

Selenium (Se) is an essential trace element for humans and animals (Tan JA et al., 2002; Thomson CD, 2004; Fordyce FM, 2013), which can exert positive influence on organisms at moderate levels by enhancing their immunity and anti-aging capacity (Feng CX et al., 2021; Wang XQ et al., 2021). Se has a dual biological function (Li ML et al., 2020), with excessively low and high intake both capable of causing human health problems (Yang GQ et al., 1983; Bajaj M et al., 2011; Shi ZM et al., 2017; Newman R et al., 2019; Liu NN et al., 2021; Li XZ et al., 2023). The Se in humans

First author: *E-mail address*: 369517099@qq.com (Yong-chun Li).

* Corresponding author: *E-mail address*: houhongbing@sina.com.cn (Hong-bing Hou).

Literary editor: Li-qiong Jia
doi:10.31035/cg2024037
2096-5192/© 2026 China Geology Editorial Office.

primarily comes from the food chain, while the Se in plants (crops) is mainly from the soil (Dinh QT et al., 2018). Therefore, the geological genesis of soil Se has been a hot research topic.

The Hetao Plain is a major grain production base in northern China, where the research, conservation and development of land resources have always been the vital focus (Li SB et al., 2023). Despite the low soil content of Se in the plain, which is located at the edge of the low Se soil zone proposed by Tan JA (1989), relevant investigations have indicated local presence of Se-rich soils in Hetao region. Wang ZJ and Gao YX (2001) attributed the controlling factors of the low Se zone to the hydrologic migration processes including soil organic matter (SOM) and leaching, as well as the soil forming rocks and weathered material with low Se content. Some other scholars (Sun GX et al., 2016) indicated that the Se volatilization in low Se zone soil is equivalent to the input of atmospheric wet deposition. However, some Se-rich soil areas have been found in the low Se zone, and it is generally acknowledged that the underlying or surrounding parent rocks are the primary source of soil Se (Blazina T et al., 2014). Since the Hetao region is deposited with exceptionally thick Quaternary strata, and the high Se zone is far away from the bedrock exposure area, it is difficult to attribute the source of soil Se to the bedrock. Currently, the origin of local Se-rich soil in the Hetao region still lacks reasonable explanation.

To clarify the geological source and biological effects of soil Se in Hetao Plain, a 1∶50 000 scale geochemical survey of land quality was performed in Hesheng Township, Wuyuan County, the hinterland of the Hetao Plain. A series of soil and crop samples were collected, with which the spatial distribution characteristics and influencing factors of soil Se in the study area were investigated. The geological genesis of Se anomaly zone was explored by comparing the chemical weathering intensity and the rare earth elements (REE) distribution pattern between the high Se zone and other surrounding parent materials. Additionally, the development and utilization potential of Se-rich soil resources was discussed by comparing the corresponding statistics of Se-rich soil and crops. The objectives of this study are presented as follows: (1) To identify the controlling factors of soil Se in the study area; (2) to investigate the geological origin of soil Se anomaly zone; (3) to evaluate the biological effects of Se and promote the development and utilization of Se-rich land.

2. Materials and methods

2.1. Study area

The study area, with geographical coordinates 108°16'24"–108°37'50"E, 41°3'56"–41°11'5"N, is situated in the hinterland of the Hetao Plain, which neighbors the "几"-shaped bend of the Yellow River in the south and adjoins the Langshan Mountain, the western end of Yinshan Mountains, in the north. Regarding geotectonic units, the study area is located in the Yinshan–Tianshan latitudinal tectonic belt, which is an inland faulted basin covered by loose quaternary strata, with thick lacustrine strata deposited in the lower part and extensive alluvial-lacustrine sediments distributed on the surface. Moreover, there are also small areas of Yellow River modern alluvia (floodplain), lacustrine sediments (Muyang Lake), as well as piedmont diluvia of different geological periods. The terrain of the study area is flat, approximately 80% of which is cultivated land, and the rest consists of scattered construction, forest and grass lands, along with interwoven road network and irrigation water network. The study area adopts flood irrigation from the Yellow River. Naturally, the irrigation water is discharged to the Wujia River (main drainage channel of the irrigation area), and flows from west to east into the Wuliangsu Lake.

2.2. Sample collection

This survey research is divided into two parts. At first, a 1∶50 000 scale geochemical soil survey was conducted in Hesheng Township, Wuyuan County. Following the *Specification of Land Quality Geochemical Assessment* (DZT 0295-2016), totally 1985 surface soil samples were collected at a sampling density of 6–8/km^2, and a control area of approximately 269 km^2. Meanwhile, 120 groups of crop and root soil samples were collected, including 48 groups of sunflower seed samples, 42 groups of corn samples and 30 groups of zucchini (various zucchini, whose edible part is seeds) seed samples. Secondly, to investigate the geological genesis of soil Se in the Se anomaly zone, 6 vertical profiles (0–2 m) were designed in areas with varying content levels of surface soil Se, and the deep soil samples were continuously collected at about 20 cm spacing. A series of surface and deep soil profile samples were collected from typical parent material areas (including the Yellow River Floodplain, modern lacustrine sediments and piedmont diluvia) outside the geochemical survey area. Fig. 1 shows the specific sampling sites.

2.3. Sample analysis

Sample testing was performed by Hebei North China Geological Exploration Ecological Resources Monitoring Center Co., Ltd. For the particle size analysis of soil samples, the Mastersizer 2000 (UK) was applied. After natural air-drying and removal of stones, plant roots, etc., the soil samples were crushed, passed through a 10-mesh screen and measured for pH with a pH meter (PHS-3C, Shanghai, China). Subsequently, the samples were passed through a 60-mesh screen and determined for SOM with a high-frequency infrared carbon and sulfur analyzer (HCS-801, Sichuan, China). The remaining samples were crushed to 200 mesh in agate jar to measure the contents of other elements in soil. Among them, the constant elements were assessed by X-ray fluorescence spectrometry (PW4400, Netherlands), nitrogen (N) was determined with an automatic Kjeldahl analyzer (K1100, Shandong, China), phosphorus (P) was determined with an ICP-OES analyzer (iCAP7400, USA), Se was identified by atomic fluorescence spectrometry (SK-Ruixi, Beijing, China), and REEs were assessed using an inductively coupled plasma mass spectrometer (XSeries2, USA). The

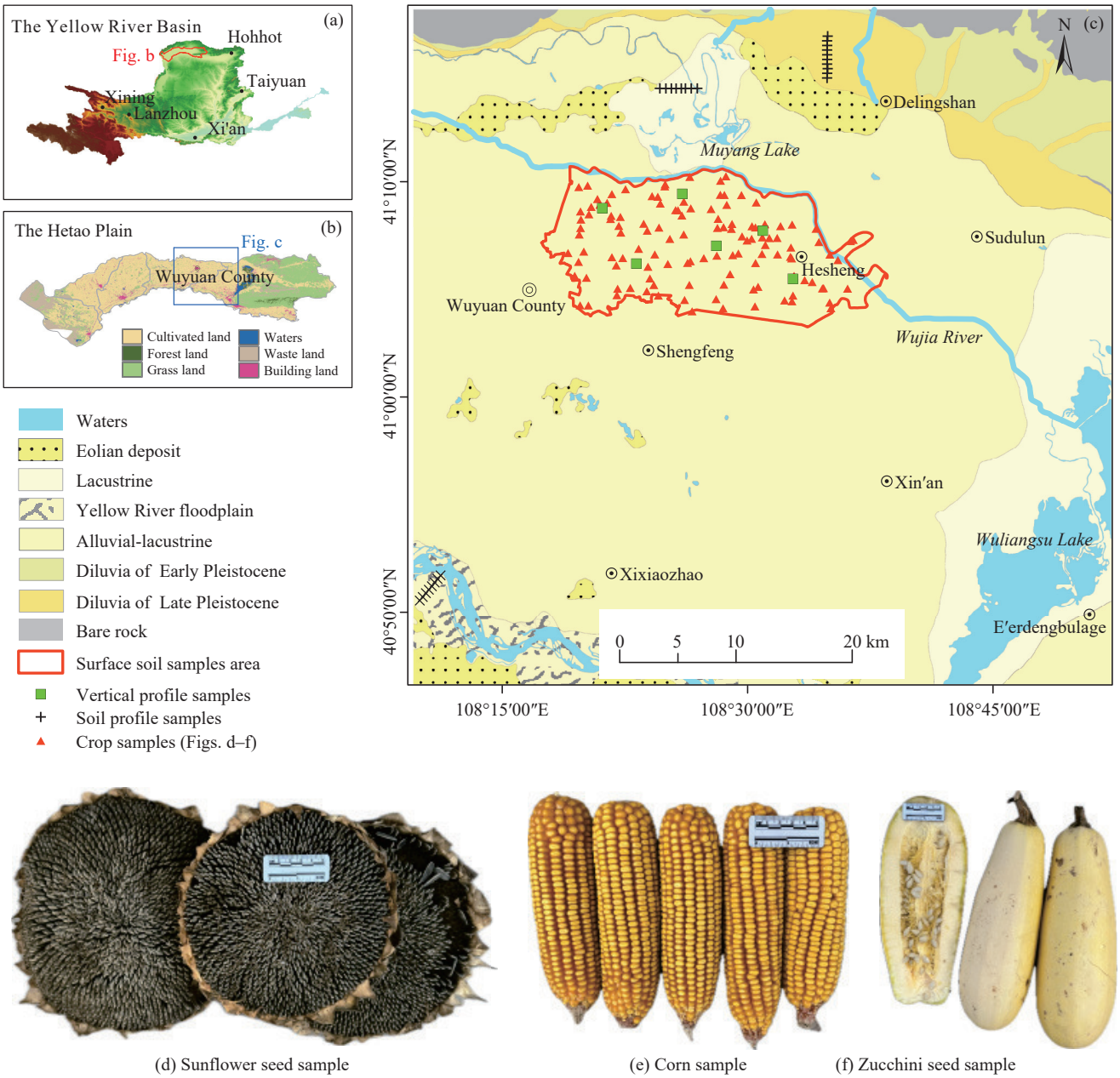

(d) Sunflower seed sample (e) Corn sample (f) Zucchini seed sample

Fig. 1. a–Location of the Hetao Plain in the Yellow River Basin; b–location of study area in Hetao Plain; c–geological map and sampling location of the study area; d–f–crop samples.

crop samples were naturally air-dried, hulled, cleaned in the laboratory with deionized water and crushed into powder. The dry samples were weighed into the microwave digestion tank, added with subboiling nitric acid along with MOS grade H_2O_2, and later placed into a microwave digestion system for digestion. After the reaction, the digestion tank was removed, placed on an acid discharger and evaporated to a small volume. Next, the sample solutions were cooled, transferred to 10 mL colorimetric tubes, filled with ultra-pure water and shaken well. Finally, each 2.5 mL of solution was placed into a colorimetric tube, added with 1 mL of hydrochloric acid, filled with ultra-pure water to 5 mL, shaken well and subjected to atomic fluorescence spectrometry (SK-Ruixi, Beijing, China) for crop Se determination. In the soil sample analysis, the accuracy and precision of test results were controlled by inserting national first-class standard substances or replicate samples. Then, 48 and 191 national first-class standard substances were inserted for accuracy and precision control, respectively, with the accuracy and precision pass rates being 100%. In the case of crop analysis, 4 national first-class standard substances, 30 replicate samples and 30 external test samples were inserted. The pass rates of accuracy, replicate analysis and external test were all 100%. Based on the quality control results, the accuracy and precision of all sample test analyses were within the permissible ranges and satisfied the specification requirements.

2.4. Data processing and analysis

Descriptive statistics of samples and data analysis were

accomplished using the Excel 2016 (Microsoft) and SPSS 22.0 (IBM), while map drawing was accomplished using the GeoChem Studio 3.5 and ArcGIS 10.2.

3. Results

3.1. Geochemical characteristics of soil Se and other elements (compounds)

The surface soil in the study area exhibited alkaline pH values ranging from 8.0 to 10.5, with a median of 8.9. The Se content ranged from 0.07 mg/kg to 0.72 mg/kg, with a mean of 0.24 ± 0.06 mg/kg and a variation coefficient of 0.26, which was higher than the soil background values of Inner Mongolia (0.16 mg/kg; Hou QY et al., 2020) and Hetao Irrigation District (0.20 mg/kg; Wang XK et al., 2007). The concentration factor values were 1.48 and 1.21, respectively, indicating relative enrichment of soil Se in the study area. Table 1 presents the content characteristics of other chemical indicators.

The correlation coefficients between Se and constant elements in soil were calculated (Table 2). Se was significantly correlated with Al, Fe and SOM, while negatively related to Si, Na and pH. Se is easily adsorbed by Al, Fe and other metal oxides, which tends to form relatively insoluble complexes and compounds with sesquioxides (Fe_2O_3, MnO_2, Al_2O_3), or be captured by metal hydroxides (especially $Fe(OH)_3$) (Yang ZF et al., 2012). Since Al, Fe and other metal oxides are one of the positively charged colloidal minerals in soil, the Se oxyanions can form stable internal complexes with them and precipitate (Muller J et al., 2012; He YZ et al., 2018; Farooq MR et al., 2023). As a representative biophile element, Se is easily enriched in the SOM-rich soil environment. Soil SOM shows adsorption capacity, which easily undergoes coordination reaction with Se to form chelates, therefore sequestrating Se in the soil (Wang QY et al., 2016; Xiao KC et al., 2020).

Table 1. Statistical parameters of soil elements in the study area (*n*=1985).

Indicator	Minimum	Maximum	Mean	Median	Variation coefficient
Se/(mg/kg)	0.07	0.72	0.24	0.24	0.26
pH	8.0	10.5	–	8.85	–
SOM/%	0.02	4.21	1.16	1.16	0.32
SiO_2/%	49.1	68.7	55.8	55.5	0.05
Al_2O_3/%	8.87	15.78	12.23	12.30	0.09
Fe_2O_3/%	2.75	6.65	4.95	4.98	0.14
MgO/%	1.48	4.27	2.79	2.82	0.11
CaO/%	1.37	10.47	8.49	8.50	0.09
Na_2O/%	0.83	3.73	1.24	1.22	0.20
K_2O/%	2.00	3.42	2.56	2.56	0.08

Note: – indicates statistical insignificance.

From a perspective of spatial distribution (Fig. 2), the soil Se and the aforementioned elements or compounds were highly consistent in spatial distribution, all exhibiting east-westward high anomalies (Si and Na exhibited low anomalies) in the slightly northern central part of the study area. The spatial distribution of soil Se in the study area was controlled by constant oxides and SOM.

3.2. Vertical distribution characteristics of soil Se

According to the six profiles excavated in the study area, the surface soil was dark gray-gray black loam or heavy loam, while the structure below the surface soil was basically sand-clay interlayers (Fig. 3). It is indicated that the soil genesis in the study area has undergone alternating evolution of strong and weak hydrodynamic deposition. The clay layer was mostly brick red or dark red in color, with tight texture and crumbled structure, while the sand layer was mostly grayish yellow-dark yellow in color. For the vertical distribution, Se content declined spirally from top to bottom, which was consistent with the three-dimensional stratification structure of soil profiles, exhibiting high Se in the clay layer and low Se in the sand layer.

With the profile No. CPM52 as an example (Fig. 4), the vertical distribution characteristics of Se were similar to those of horizontal distribution, exhibiting a good consistency with constant oxides (e.g. Si, Al and Fe) and SOM. In addition, the vertical variation of Se was consistent with both the average particle diameter and clay content of soil. When the soil particle diameter was small, the proportion of clay components remained high, thereby facilitating Se enrichment; conversely, when the particle diameter was large, the proportion of sand and gravel components increased, which hindered Se sequestration. The soil Al/Si ratio can reflect the variation of soil sediment size (Zhu LX et al., 2002; Xia W et al., 2023), with higher Al content and lower Si content suggesting finer soil particles and higher clay content. Therefore, the correlation between Se and constant oxides actually reflects the Se adsorption control by soil clay minerals.

3.3. Characteristics of crop Se contents

The characteristic parameters of different crops were explored in terms of Se content and BCF (BCF = Se in crop/Se in root soil) (Table 3). The results suggested that the crops produced in the study area exhibited higher content levels than similar crops in China, with the Se content and BCF rankings all characterized by zucchini seeds > sunflower seeds > corn. The mean Se contents in root soil corresponding to the aforementioned crops were 0.28 ± 0.08 mg/kg, 0.28 ± 0.07 mg/kg and 0.27 ± 0.07 mg/kg, respectively, with no

Table 2. Correlation coefficients between Se and other elements in soil (*n*=1985).

	SOM	SiO_2	Al_2O_3	Fe_2O_3	MgO	CaO	Na_2O	K_2O	pH
Se	0.49^{**}	-0.55^{**}	0.53^{**}	0.55^{**}	0.57^{**}	0.48^{**}	-0.35^{**}	0.54^{**}	-0.212^{**}

Note: ** indicates significant correlation at the 0.01 level (two-tailed).

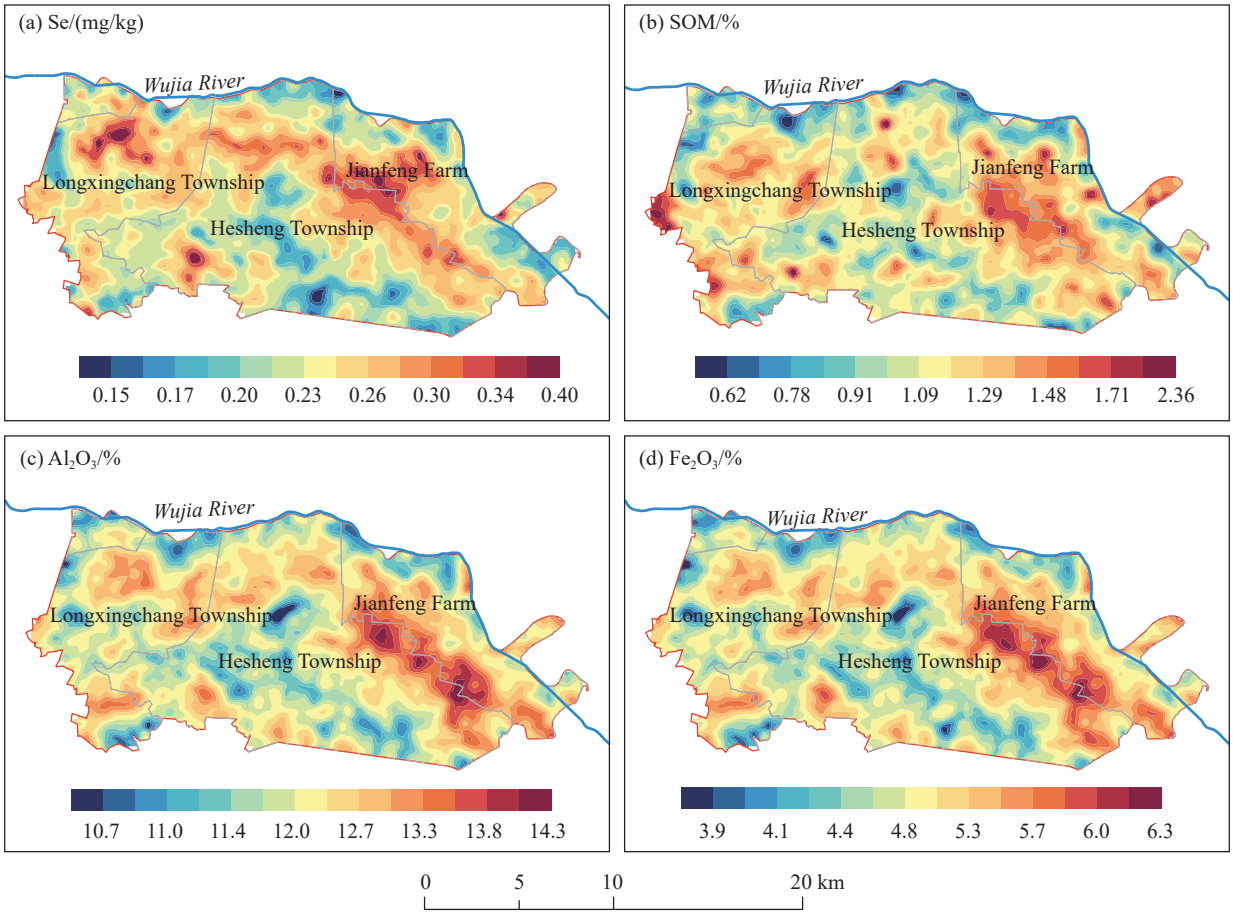

Fig. 2. Spatial distribution map of soil Se and other chemical compounds.

significant differences. This demonstrated that the foremost factor influencing the crop absorption of Se was the crops themselves. Previous research has also revealed that families like Leguminosae, Compositae (sunflower) and Cruciferae had strong abilities to accumulate and transform soil Se, while the soil Se absorption capacities of cereal crops like wheat and corn remained relatively weak (El MAF et al., 2014). The zucchini seeds collected in this study were the product of a special zucchini variety for seed harvesting. Despite the limited number of the collected samples, the ultrahigh Se content and ultrahigh BCF of crops indicate that they are a kind of SE super-accumulating plants with strong Se absorption and transformation abilities, deserving attention in the future development of Se-rich agricultural products.

3.4. Provenance indication by different parent material characteristics

3.4.1. Provenance characterization by chemical weathering intensity

The chemical index of alteration (CIA) and the Na_2O/K_2O molar ratio are common indices used for evaluating the chemical weathering intensity (Nesbitt HW et al., 1982). CIA, as the ratio of Al_2O_3 to unstable oxides, shows the intensity of feldspar weathering into clay minerals, where the element redeposition after migration is absent. Therefore, it excellently reflects the chemical weathering at the time of sediment formation, rather than the later environmental changes (Ling CH et al., 2015). Due to the environmental disparity, the soils formed in different provenance areas have undergone different chemical weathering stages, and therefore the characteristics of soil CIA also have certain indicative significance for provenance. CIA is also impacted by geomorphic features, vegetation and anthropogenic activities. The Na_2O/K_2O ratio is a measure of plagioclase weathering intensity in the samples, which is inversely proportional to the intensity of weathering. Thus, Na_2O/K_2O ratio is generally employed to demonstrate the prediction accuracy of provenance weathering intensity by CIA. CIA = $[Al_2O_3/(Al_2O_3+CaO^*+K_2O+Na_2O)] \times 100$, where all are the molar numbers of oxide molecules, and CaO* indicates the Ca content in sediment silicate minerals, excluding the CaO content in carbonate and phosphate. The method proposed by McLennan SM (1993) was used for calibration. If $n(CaO) < n(Na_2O)$, $n(CaO)$ was applied as CaO*; otherwise, $n(Na_2O)$ was used as CaO*. Fedo CM et al. (1995) found that a ClA value ranging between 50 and 60 reflected the elementary chemical weathering under cold and dry climates; in addition, a CIA value ranging between 60 and 80 suggested the moderate chemical weathering under warm and humid conditions; CIA values which were greater than 80 reflect strong chemical weathering under hot, humid tropical and subtropical conditions.

The soil CIA values of parent materials in and around the

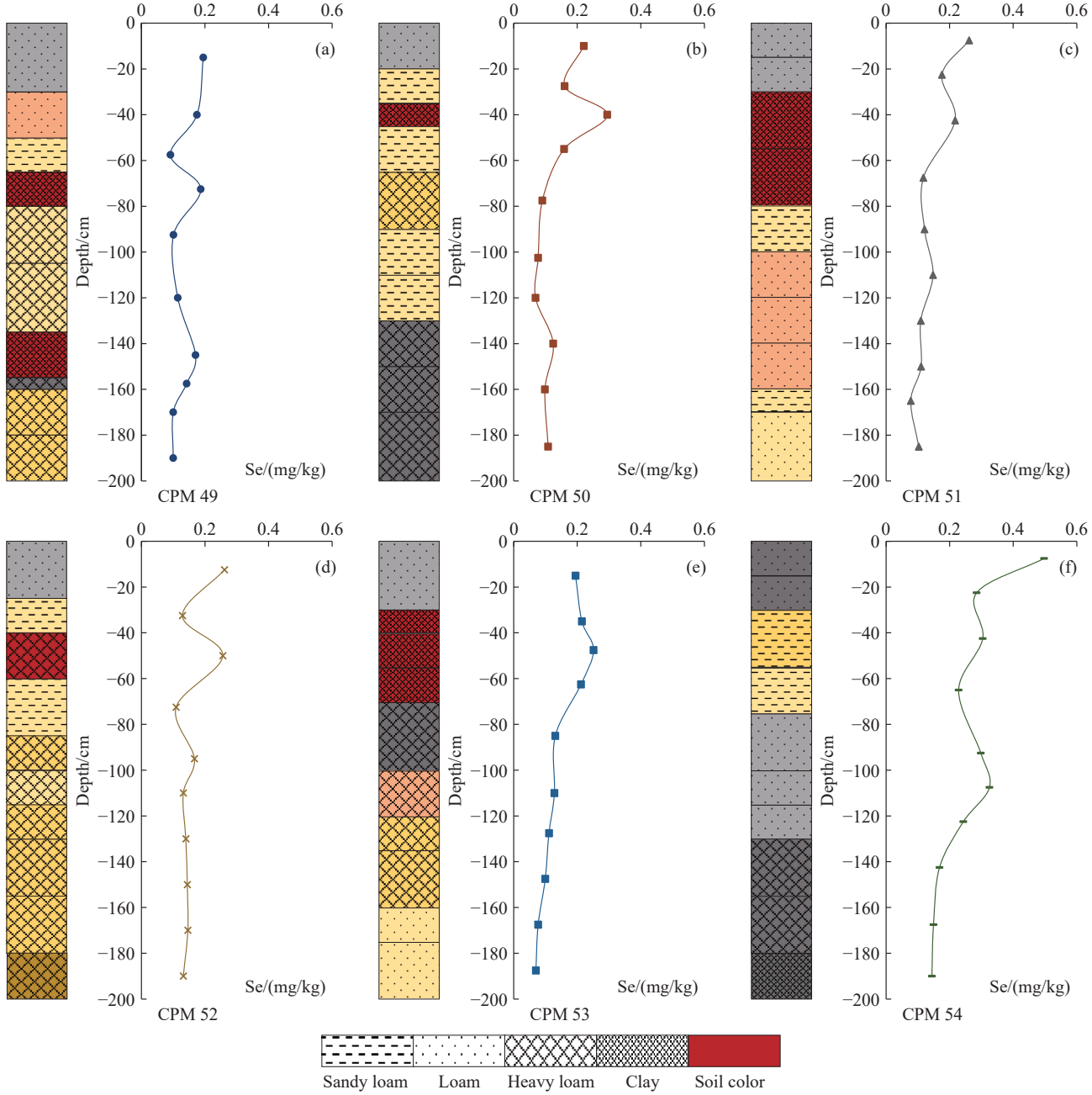

Fig. 3. Sketch map of soil profile patterns and variation trend of Se (CPM stands for the soil profile number).

study area were calculated, and the CIA and Na_2O/K_2O values of sample data were projected into the coordinate system (Fig. 5). A significant negative correlation between soil CIA and Na_2O/K_2O ratio was present in different parent material areas, revealing the accuracy of CIA in showing the weathering intensity and its applicability in the study area. The CIA values of soil samples in the study area ranged from 48.12 to 68.98, with a mean of 64.97, which was higher than the mean value in the upper continental crust (UCC) (47.92) and slightly lower than the mean value in Luochuan loess (72.14; Chen YY et al., 2008). Moreover, this indicated that the soils in the study area had experienced moderate chemical weathering under relatively warm and humid conditions. The narrow range of soil CIA values also indicates the development and formation of soils (parent materials) in the study area under a stable climatic environment. The soil CIA comparison among different parent materials found that the study area ≈ Yellow River floodplain > lacustrine parent material > diluvial parent material. The CIA of soils developed from piedmont diluvial parent material ranged between 48.20 and 55.09, with a mean of 52.16, which was close to the mean value in the UCC. This demonstrated that they had experienced elementary chemical weathering under cold and dry climates. Thus, it could be inferred that the soils in the study area originated primarily from the Yellow River alluvia, whose soil CIA was close to the study area. As shown in Fig. 5b, the Se contents in soils from different parent materials were positively correlated with CIA, and the correlation coefficient for the study area was 0.49. This suggested that strong chemical weathering could accelerate

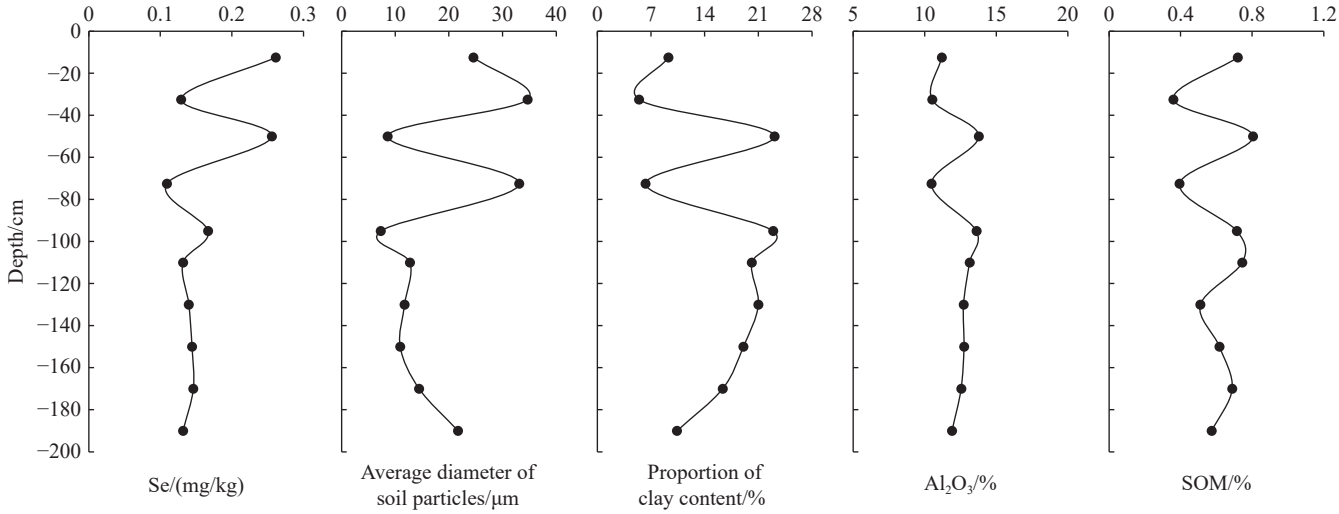

Fig. 4. Variation trends of Se and other indicators in soil vertical profiles.

Table 3. Statistics of characteristic parameters of different crops.

Crop and sample size	Se content range /(mg/kg)	Mean Se /(mg/kg)	National mean /(mg/kg)	BCF range	Mean BCF
Sunflower seeds (*n*=48)	0.03–0.50	0.12	0.058	0.11–1.46	0.41
Corn (*n*=42)	0.03–0.26	0.07	0.035	0.10–0.81	0.25
Zucchini seeds (*n*=30)	0.07–0.58	0.22	0.028	0.30–2.62	0.80

Note: National mean values are from the *6th Edition of China Food Composition Tables (Standard Edition)*.

the soil-forming process of desilication and allitization to facilitate the Se enrichment.

3.4.2. Provenance indication by REE partitioning characteristics

Considering their similar chemical properties, REEs undergo certain fractionation in different geological processes, but they are still symbiotic in nature (Liu DS, 1985; Ran Y and Liu Z, 1994; Yang SY and Li CX, 1999). Thus, the REE partitioning pattern can well reflect the soil provenance attributes. Surface soil is easily impacted by anthropogenic activities, while deep soil is more indicative of the original characteristics of parent materials, and deep soil samples were used to represent the parent materials. The REE characteristic parameters of parent materials in the high Se zone and its periphery were statistically assessed (Table 4). The partition patterns of mean REEs normalized to UCC and the scatter diagram of ∑REE *vs*. LREE/HREE were plotted (Fig. 6), reflecting the differences among various parent materials (Chen XL et al., 2017; Han L et al., 2019).

The results were presented as follows: (1) The LREE/HREE of all samples ranged from 7.51 to 10.07, indicating that the parent materials in the study area and its periphery were significantly differentiated into light and heavy REEs, which exhibited relative enrichment of light REEs, exhibiting consistency with the “light in the north, heavy in the south” distribution characteristic of REEs in China (Wang ZW et al., 2022). (2) The REE distribution in different parent materials varied, with the specific ∑REE rankings being high Se zone > lacustrine parent material ≈ floodplain > diluvial parent material. The diluvial parent material exhibited significantly lower REE than others, demonstrating that the REE fractionation had undergone different geological processes. The diluvial parent material originated primarily from the Langshan Mountain bedrock and mixed with weathered products of different lithologies, and therefore the drop points in ∑REE and LREE/HREE scatter diagrams were dispersed. (3) According to the partition patterns (Fig. 6a), the parent material of high Se zone differed somewhat from the floodplain and lacustrine parent materials. However, in the ∑REE *vs*. LREE/HREE diagram (Fig. 6b), the samples basically fell in the same areas, with fundamentally identical slopes, revealing that the parent materials in the study area originated from the sediment transport of water system. Nevertheless, it also suggests that the development and formation of soil parent materials in the study area had experienced different geological processes.

4. Discussion

4.1. Soil Se enrichment pattern in the study area

Some studies have suggested that the distribution and enrichment of Se are primarily influenced by geological background, which are especially associated with high Se strata including black rock series or mud shale (Kulp TR and Pratt LM, 2004; Ni RX et al., 2016; Yu T et al., 2018; Liao QL et al., 2020; Liu YL et al., 2022). There are also indications that the Se enrichment is associated with the secondary enrichment during soil formation, and that the Se behavior in supergene environment is significantly affected by topography, land use, soil physicochemical properties (Michele LWT et al., 2014; Dinh QT et al., 2018; Natasha et al., 2018), pH value (Fan JX et al., 2018; Farooq MR et al., 2023), SOM (Xu YF et al., 2020; Lyu CH et al., 2021), Fe, Al oxides, as well as mineral components (Gabos MB et al., 2014; Gerrad DJ et al., 2017; Wu J, 2018). Different from the

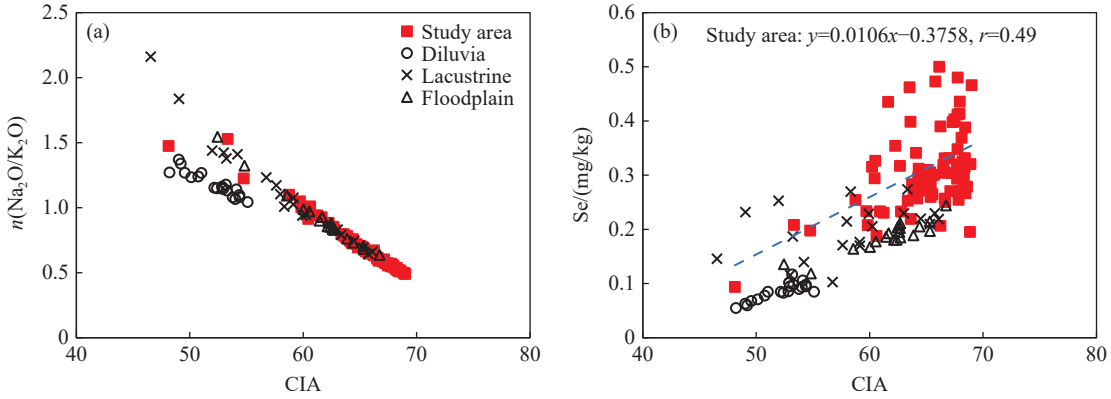

Fig. 5. Scatter diagrams of CIA *vs.* $n(Na_2O/K_2O)$ (a) and CIA *vs.* Se (b) in different soil parent materials.

Table 4. Statistical table of REE characteristics in different soil parent materials (mg/kg).

Indicator	High Se zone			Diluvia			Lacustrine			Floodplain		
	x	min	max	x	min	max	x	min	max	x	min	max
La	36.62	35.21	37.52	23.09	12.23	31.03	31.50	27.04	35.28	28.97	19.89	32.72
Ce	75.70	73.36	77.94	47.02	23.59	64.90	65.81	55.73	73.68	60.28	40.55	68.33
Pr	8.34	8.12	8.59	5.21	2.79	7.06	6.91	5.92	7.66	6.51	4.50	7.32
Nd	31.96	31.17	32.65	19.70	10.71	25.79	26.51	22.34	29.80	25.17	17.27	28.11
Sm	6.26	6.14	6.41	3.64	1.94	4.76	5.15	4.46	5.63	4.91	3.40	5.54
Eu	1.32	1.28	1.37	0.98	0.78	1.15	1.12	1.00	1.25	1.06	0.75	1.18
Gd	5.93	5.77	6.10	3.54	1.90	4.70	5.06	4.55	5.65	4.76	3.33	5.45
Tb	0.86	0.83	0.89	0.51	0.28	0.67	0.78	0.71	0.87	0.73	0.49	0.84
Dy	4.99	4.81	5.20	2.85	1.64	3.64	4.46	3.95	4.89	4.12	2.74	4.66
Ho	0.98	0.96	1.02	0.56	0.33	0.75	0.89	0.79	0.98	0.83	0.55	0.93
Er	2.90	2.83	2.98	1.62	1.00	2.07	2.53	2.28	2.85	2.40	1.58	2.76
Tm	0.44	0.43	0.47	0.23	0.15	0.30	0.36	0.32	0.40	0.34	0.23	0.38
Yb	2.93	2.84	3.04	1.62	1.10	2.05	2.49	2.24	2.76	2.41	1.61	2.77
Lu	0.42	0.40	0.45	0.24	0.16	0.31	0.36	0.32	0.40	0.35	0.23	0.39
Y	25.93	25.06	27.00	14.39	8.68	19.27	21.06	18.83	23.92	20.97	13.89	23.64
ΣREE	179.67	174.44	184.27	110.82	58.59	148.86	153.93	131.70	171.31	142.85	97.10	160.81
LREE	160.20	155.29	164.40	99.65	52.04	134.70	137.00	116.49	152.84	126.90	86.35	143.14
HREE	19.47	18.97	20.07	11.17	6.55	14.21	16.92	15.21	18.71	15.95	10.75	18.07
LREE/HREE	8.23	8.06	8.46	8.91	7.94	10.07	8.09	7.64	8.51	7.96	7.51	8.39
$(La)_N/(Yb)_N$	8.95	8.68	9.40	10.23	7.97	12.29	9.08	8.40	9.62	8.62	7.94	9.21
δEu	0.66	0.65	0.68	0.86	0.74	1.23	0.67	0.65	0.72	0.67	0.65	0.70
δCe	1.06	1.05	1.08	1.05	0.99	1.08	1.09	1.07	1.12	1.08	1.05	1.10

Note: $\delta Eu=2*(Eu)_N/[(Sm)_N+(Gd)_N]$; $\delta Ce=2*(Ce)_N/[(La)_N+(Pr)_N]$.

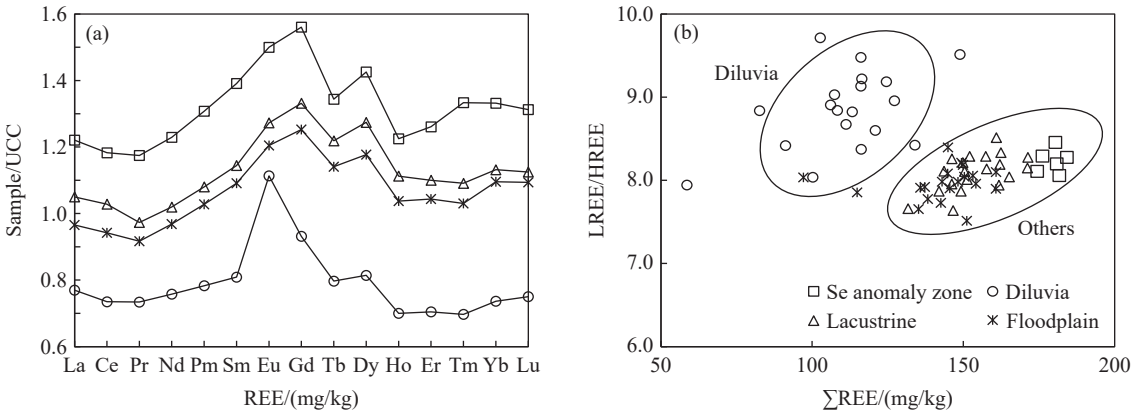

Fig. 6. Distribution patterns of REE normalized to UCC (a) and scatter diagram of ∑REE *vs.* LREE/HREE (b) in different soil parent materials.

residual slope soil, the provenance of soil elements in alluvial plain areas is a complex problem, since its parent material may be originated from weathered and denuded products of surrounding parent rocks, or may have experienced geological

processes including strong mixing, extensive transport and deposition (Ma SM et al., 2006; Yu C et al., 2022). Meanwhile, the cause may also be the superposition of secondary effects, anthropogenic inputs and multiple effects (Zhou GH, 2020), making accurate identification of dominant factors difficult, and certainly, it is unnecessary. In this study, the provenance change in soil parent material was determined and its geological genesis was only analyzed by the characteristics of soil element composition (Zhu LX et al., 2002). This provides an idea for further investigation of Se-rich soils in the surrounding regions, and also a foundation for the Quaternary geological and geochemical research and environmental geochemical assessment.

This study explored the geochemical characteristics of soil Se and other elements, and clarified that the Se enrichment was controlled by such physicochemical properties as soil clay minerals, Al, Fe and SOM. The differences among various parent materials were compared from the perspectives of chemical weathering intensity and REE distribution pattern. The results demonstrated that the parent materials in the study area originated primarily from the water system transportation and deposition, which were little influenced by the bedrock in the northern part. However, it remains difficult to clarify the intrinsic geological factors for the formation of high Al, high Fe and high Se banded anomaly zone in the study area. In a study conducted in Chengde of Hebei, Wei H et al. (2024) proposed a "channel sedimentary type" pattern of Se enrichment, providing a good referential significance for the Se distribution and origin in the study area. Based on the sand-clay interlayered structure of investigated soils, it can be observed that the development and formation of underlying parent materials have experienced alternating changes of hydrostatic sedimentation and weak hydrodynamics, and that Se tended to accumulate in clay-rich layers formed in the hydrostatic sedimentary environment. A large number of ancient river channels remain on the surface of Hetao Plain. Since the 18th century (Qing Dynasty), the mainstream of the Yellow River has shifted from northward to southward. Since then, the northward mainstream has gradually silted up and stopped flowing. After generations of agricultural reclamation and irrigation, along with several dredges and repairs, it is currently challenging to distinguish the original state of river channels from the ground. According to comparison of the geographical position of the Yellow River ancient channel proposed by Li BY (2003) (Fig. 7) with that of the high Al, high Fe and high Se zone in the study area, the distribution patterns of the high Se zone and the ancient channel were basically consistent. Therefore, it can be inferred that the origin of the banded high Se soils in the study area is also "channel sedimentary type", which may be related to the Yellow River ancient channel. During the diversion of the Yellow River, the water flow of the original channels became smaller and slower, leading to gradual silting up. During the process of changing from a hydrodynamic to hydrostatic environment, substantial clay materials were deposited, and under their adsorption effect, most elements including Se were enriched. This conclusion can also be corroborated by the aforementioned finding that the soil parent materials in the high Se zone of the study area underwent different geological processes compared with the soil-forming process of floodplain and lacustrine parent materials. That is to say, the soils in the high Se zone experienced gradual drying up of the Yellow River ancient channel, where more fine clay materials have been deposited.

4.2. Development potential of Se-enriched land resources

The ultimate goal of investigating the geochemical characteristics and geological genesis of soil Se is to serve the development and utilization of Se-enriched land resources. According to the *Delineation and Identification of Naturally Selenium-enriched Lands* (DZ/T 0380-2021) promulgated by China Geological Survey in 2021, approximately 2066.7 hectare of cultivated land in the study area has reached the Se-enrichment standard, occupying approximately 10% of the study area, whose specific distribution is in consistence with the aforementioned high Se zone. Some scholars (Zhou GH, 2020; Xu XS et al., 2022; Ren R et al., 2024) have stated that the Se-enriched lands should be assessed by comprehensively considering such production factors as soil fertility,

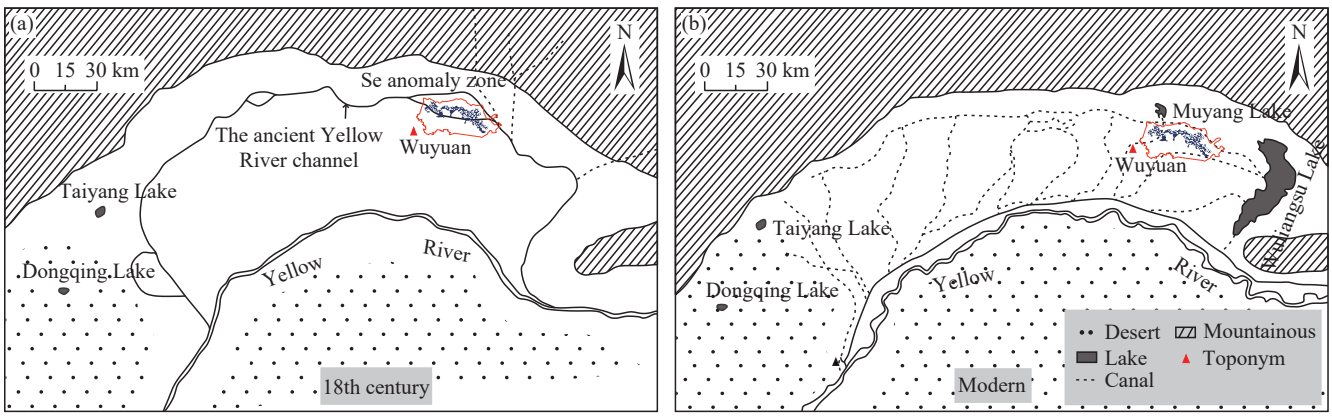

Fig. 7. Comparison of the Se anomaly zone with the geographical position of the Yellow River ancient channel. a–Course of the Yellow River in the 18th century; b–modern course of the Yellow River. The red line indicates the location of the study area; the blue area indicates the location of the selenium anomaly zone (after Li BY, 2003).

geomorphology, irrigation support and crop Se enrichment rate. Based on the above discussion, the Hetao Plain in the study area has flat terrain, irrigation support from the Yellow River and superior agricultural facilities, where the Se content is significantly related to the SOM, N, P, K and other nutrient indicators. This ensures adequate fertility of the investigated Se-enriched land and good production conditions for the development of Se-enriched land resources. Thus, the key question for determining whether the investigated Se-enriched land resources have a development potential is: Whether "qualified" Se-rich agricultural products can be produced in the Se-enriched land? The biological effects of Se need to be further evaluated.

Ideally, Se-rich soils should correspond one-to-one to Se-rich crops (Wang HY et al., 2021). Some studies have indicated that soil Se is not the only constraint of crop Se content, while factors including crop species and soil physicochemical properties have varying degrees of influence on the crop Se absorption (Reynolds RJB et al., 2020; Wang RQ et al., 2022; Li YC et al., 2024), and the dominant factor varies greatly across different regions. Based on the results of this study (Table 5), the Se contents in all types of crops were significantly associated with the Se in root soil. Except for the Se in sunflower seeds, which was also positively related to the soil SiO_2 and pH, the Se contents of other crops were little correlated with other soil elements (compounds). In combination with Section 3.3, it can be concluded that the crop species and soil Se content constitute the main factors influencing crop Se content in the study area. It has been reported (Yang ZF et al., 2012) that the pH environment largely determines the actual chemical form of Se in soil. In well-aerated alkaline soil, Se primarily exists in the form of selenate with higher solubility, which is therefore also a vital influencing factor of crop Se content. However, in this study area, crops other than sunflower seeds did not exhibit such relationship, which is caused by the relatively narrow range of soil pH and the similar soil acid-base environment in the study area. Thus, although soil pH in the study area is not the primary factor responsible for the difference in crop Se content, the generally alkaline soil environment is beneficial for the crop Se absorption.

The evaluation of Se-enriched land resources needs to concentrate on the crop Se levels (Zhou F et al., 2022). Inner Mongolia, where the study area is located, has not promulgated relevant standards for Se-rich agricultural products. The production and utilization potential of the investigated Se-enriched land was discussed following the standards for *Selenium-enriched Corn* (GB/T 22499-2008) and the *Guangxi Requirements on Selenium Content Classification of Selenium-rich Agricultural Products* (DB45/T 1061-2014) (both sunflower seeds and zucchini seeds can be used for oil production as oil crops). As displayed in Table 6, all the crops collected in this study had high Se enrichment rates, and the Se enrichment rates of crops growing in the Se-rich areas exceeded 92.9%, which were higher than those of corresponding crops in the non-Se-rich areas. Corn exhibited the largest difference, followed by sunflower seeds, while the Se contents of all zucchini seed samples exceeded the corresponding Se enrichment standards, with a Se enrichment rate of 100%. Moreover, this result also greatly suggests that the investigated Se-enriched land has a high potential for Se-rich crop production. Combined with Section 3.3, it can be inferred that the soil Se demands vary from crop to crop. For example, Se-rich zucchini seeds can be grown within the entire study area owing to their extraordinarily Se absorption capacity. In terms of sunflower seeds, the standard can also be appropriately lowered to expand the range of Se-enriched land resources. Furthermore, this requires determination of the adequate lower threshold for soil Se by further establishing the fitted equation between crop Se and soil Se, which is also the direction of our following research.

5. Conclusions

In this study, the distribution characteristics of Se in soils and crops in the hinterland of Hetao Plain, Inner Mongolia are systematically investigated. The influencing factors of soil Se distribution are assessed, and the geological genesis of Se anomaly zone and the development and utilization potential of Se-rich soil are discussed. The results demonstrate that the soil Se in the study area is higher than the background values of Inner Mongolia and Hetao Plain, with Se enrichment in local soils under specific conditions.

(i) The spatial distribution of soil Se in the study area is restricted by factors including soil clay minerals, constant

Table 5. Correlation coefficients between crop Se and soil elements.

	Se	SiO_2	Al_2O_3	Fe_2O_3	MgO	CaO	Na_2O	K_2O	SOM	pH
Se-corn (n=42)	0.48**	0.07	−0.07	0.13	0.01	0.08	−0.18	0.04	−0.15	0.03
Se-sunflower seeds (n=48)	0.44**	0.34*	−0.25	−0.02	−0.15	−0.2	−0.08	−0.05	−0.24	0.29*
Se-zucchini seeds (n=30)	0.44*	0.08	−0.17	−0.16	0.06	−0.12	0.26	−0.25	−0.15	0.01

Note: "**" indicates significant correlation at the 0.01 level (two-tailed); "*" indicates significant correlation at the 0.05 level (two-tailed).

Table 6. Statistics on selenium enrichment rate of crops.

Crop	Se-enriched area				Non-Se-enriched area			
	Mean Se/(mg/kg)	Number of samples	Number of Se-rich samples	Se enrichment rate/%	Mean Se/(mg/kg)	Number of samples	Number of Se-rich samples	Se enrichment rate/%
Corn	0.10	14	13	92.9	0.05	28	16	57.1
Sunflower seeds	0.17	18	17	94.4	0.10	30	24	80.0
Zucchini seeds	0.31	9	9	100	0.18	21	21	100

oxides and SOM. The distribution of high Se soils exhibits a banded pattern planarly, consistent with the distribution of soil clay components vertically.

(ii) Comparison of soil chemical weathering intensity and REE distribution pattern reveals that the investigated soil parent materials are primarily originated from the water system transportation. By combining the characteristics of soil sedimentary sequences in the study area with the location of the Yellow River ancient channel, it is suggested that the enrichment pattern of banded high Se soils in the study area is "channel sedimentary type".

(iii) The crops in the study area exhibit higher Se contents than similar crops in China, and crop species and soil Se content constitute the main influencing factors of crop Se content. The seed Se content and Se enrichment rate of crops grown in Se-rich areas are significantly higher than those in non-Se-rich areas. In addition, this indicates that the investigated Se-enriched land has a high potential for Se-rich crop production.

(iv) This study proposes a Se enrichment pattern for Se-rich soils in low Se zone, providing a scientific foundation for the development and utilization of Se-enriched lands. However, different crops vary in their soil Se demands. For example, Se-rich zucchini seeds can be produced as long as the soil Se content reaches a certain level owing to their extraordinarily Se absorption capacity. Therefore, to develop Se-enriched lands, it is essential to determine the adequate lower threshold for soil Se by further establishing the fitted equation between crop Se and soil Se.

CRediT authorship contribution statement

Yong-chun Li and Hong-bing Hou conceived the presented idea. Yong-chun Li prepared the manuscript. Guo-dong Chen and Yu-chun-zi Du collected soil and crop samples in the field and processed geochemical data. Xue-zhen Li drew some of the figures. Jiu-fen Liu and Hong-bing Hou supervised the findings of this work. All authors discussed the results and contributed to the final manuscript.

Declaration of competing interest

The authors declare no conflict of interest.

Acknowledgment

This research was financially funded by Science and Technology Innovation Foundation of Comprehensive Survey & Command Center for Natural Resources (KC20220006) and the projects of China Geological Survey (DD20243000, DD20191015). Part of the elements in Fig.1a was provided by National Cryosphere Desert Data Center.

References

Bajaj M, Eiche E, Neumann T, Winter J, Gallert C. 2011. Hazardous concentrations of selenium in soil and groundwater in North-West India. Journal of Hazardous Materials, 189(3), 640–646. doi: 10.1016/j.jhazmat.2011.01.086.

Blazina T, Sun YB, Voegelin A, Lenz M, Berg M, Winkel LHE. 2014. Terrestrial selenium distribution in China is potentially linked to monsoonal climate. Nature Communications, 5(Sep.), 4717. doi: 10.1038/ncomms5717.

Chen XL, Song YG, Li JC, Fang H, Li ZZ, Liu XM, Li Y, Orozbaev R. 2017. Size-differentiated REE characteristics and environmental significance of aeolian sediments in the Ili Basin of Xinjiang, China. Journal of Asian Earth Sciences, 143, 30–38. doi: 10.1016/j.jseaes.2017.03.030.

Chen YY, Li XS, Han ZY, Yang SY, Wang YB, Yang DY. 2008. Chemical weathering intensity and element migration features of the Xiashu loess profile in Zhenjiang, Jiangsu Province. Journal of Geographical Sciences, (3), 341–352. doi: 10.1007/s11442-008-0341-9.

Dinh QT, Cui ZW, Huang J, Tran TAT, Wang D, Yang WX, Zhou F, Wang MK, Yu DS, Liang DL. 2018. Selenium distribution in the Chinese environment and its relationship with human health: A review. Environment International, 112, 294–309. doi: 10.1016/j.envint.2017.12.035.

El MAF, Reynolds RJB, Prins CN, Lindblom SD, Cappa JJ, Fakra SC, Pilon-Smits EAH. 2014. Analysis of selenium accumulation, speciation and tolerance of potential selenium hyperaccumulator Symphyotrichum ericoides. Physiologia Plantarum, 152(1), 70–83. doi: 10.1111/ppl.12149.

Fan JX, Zeng Y, Sun JX. 2018. The transformation and migration of selenium in soil under different Eh conditions. Journal of Soils and Sediments, 18(9), 2935–2947. doi: 10.1007/s11368-018-1980-9.

Farooq MR, Zhang ZZ, Yuan LX, Liu XD, Rehman A, Bañuelos GS, Yin XB. 2023. Influencing factors on bioavailability and spatial distribution of soil selenium in dry semi-arid area. Agriculture, 13(3), 1–17. doi: 10.3390/agriculture13030576.

Fedo CM, Nesbitt HW, Young GM. 1995. Unravelling the effects of potassium metasomatism in sedimentary rocks and paleosols, with implications for paleoweathering conditions and provenance. Geology, 23(10), 921–924. doi: 10.1130/0091-7613(1995)023<0921:UTEOPM>2.3.CO;2.

Feng CX, Liu S, Coulson IM. 2021. Lithological and Si-O-S isotope geochemistry: Constraints on the origin and genetic environment of the selenium (Se)-rich siliceous rocks in Enshi, Hubei Province, China. Acta Geochimica, 40(1), 89–105. doi: 10.1007/s11631-020-00442-2.

Fordyce FM. 2013. Selenium deficiency and toxicity in the environment. In: Selinus O (ed.). Essentials of Medical Geology. Dordrecht, Springer, 375–416. doi: 10.1007/978-94-007-4375-5_16.

Gabos MB, Alleoni LRF, Abreu CA. 2014. Background levels of selenium in some selected Brazilian tropical soils. Journal of Geochemical Exploration, 145, 35–39. doi: 10.1016/j.gexplo.2014.05.007.

Gerrad DJ, Boris D, Peter G, Pia G, Deyan P, Steve PM, Sonia IS, Pete S, Lenny HEW. 2017. Selenium deficiency risk predicted to increase under future climate change. Proceedings of the National Academy of Sciences of the United States of America, 114(11), 2848–2853. doi: 10.1073/pnas.1611576114.

Han L, Hao QZ, Qiao YS, Wang L, Peng SZ, Li N, Gao XB, Fu Y, Xu B, Gu ZY. 2019. Geochemical evidence for provenance diversity of loess in southern China and its implications for glacial aridification of the northern subtropical region. Quaternary Science Reviews, 212, 149–163. doi: 10.1016/j.quascirev.2019.04.002.

He YZ, Xiang YJ, Zhou YY, Yang Y, Zhang JC, Huang HL, Shang C, Luo L, Gao J, Tang L. 2018. Selenium contamination, consequences and remediation techniques in water and soils: A review. Environmental Research, 164, 288–301. doi: 10.1016/j.envres.2018.02.037.

Hou QY, Yang ZF, Yu T. 2020. Soil Geochemical Dataset of China. Beijing, Geological Publishing House, 2553–2850 (in Chinese).

Kulp TR, Pratt LM. 2004. Speciation and weathering of selenium in upper Cretaceous chalk and shale from South Dakota and Wyoming, USA. Geochimica et Cosmochimica Acta, 68(18), 3687–3701. doi: 10.1016/j.gca.2004.03.008.

Li BY, Ge QS, Zheng JY. 2003. The evolution of the Yellow River channel in the Inner Mongolia Houtao Plain over the past 2000 years. Acta Geographica Sinica, 58(2), 239–246 (in Chinese with English abstract).

Li ML, Yang BY, Xu KY, Zheng DS, Tian JC. 2020. Distribution of Se in the rocks, soil, water and crops in Enshi County, China. Applied Geochemistry, 122, 104707. doi: 10.1016/j.apgeochem.2020.104707.

Li SB, Yang LG, Xiong WL, Ma ZC, Yuan HW, Duan JX. 2023. Speciation of selenium in the selenium-rich cultivated land in Linhe District, Bayannur City, Inner Mongolia and its influencing factors. Geophysical and Geochemical Exploration, 47(2), 477–486 (in Chinese with English abstract). doi: 10.11720/wtyht.2023.1010.

Li XZ, Hou QY, Duan YR, Li YC, Lin K, Li BK, Sheng WK, Wang YL, Su RLG, Gu ZL, Yu T, Tang QF, Yang ZF. 2023. Soil selenium enrichment in the Loess Plateau of China, Geogenic evidence, spatial distribution, and its influence factors. Chemosphere, 340, 139846. doi: 10.1016/j.chemosphere.2023.139846.

Li YC, Liu JF, Li XZ, Zhang D, Chen GD, Du YCZ, Zhou WH. 2024. Selenium occurrence characteristics and bioavailability of soil in the hinterland of the Hetao Plain. Environmental Science, 45(11), 6734–6744 (in Chinese with English abstract). doi: 10.13227/j.hjkx.202311175.

Liao QL, Cui XD, Huang SS, Huang B, Ren JH, Gu XY, Fan J, Xu HT. 2020. Element geochemistry of selenium-enriched soil and its main sources in Jiangsu Province. Geology in China, 47(6), 1813–1825 (in Chinese with English abstract). doi: 10.12029/gc20200617.

Ling CH, Long J, Jia YL, Hong YJ, Xu CQ, Wang PL. 2015. Geochemical characteristics and palaeoclimate significance of the Quaternary laterite of Tutan section in Poyang Lake region, northern Jiangxi Province. Journal of Palaeogeography (Chinese Edition), 17(5), 699–708 (in Chinese with English abstract). doi: 10.7605/gdlxb.2015.05.058.

Liu DS. 1985. Loess and Environment. Beijing, Science Press, 256–264 (in Chinese).

Liu NN, Wang M, Zhou F, Zhai H, Qi MX, Liu Y, Li YA, Zhang NC, Ma YZ, Huang J, Ren R, Liang DL. 2021. Selenium bioavailability in soil-wheat system and its dominant influential factors: A field study in Shaanxi Province, China. Science of the Total Environment, 770, 144664. doi: 10.1016/j.scitotenv.2020.144664.

Liu YL, Wu M, Liu R, Li J, Liu SL, Liu SY. 2022. Effect of pedogenic rock on soil selenium and its bioavailability in high geological background area. Soils, 54(4), 834–840 (in Chinese with English abstract). doi: 10.13758/j.cnki.tr.2022.04.023.

Lyu CH, Qin YJ, Zhao ZQ, üiu XW. 2021. Characteristics of selenium enrichment and assessment of selenium bioavailability using the diffusive gradients in thin-films technique in seleniferous soils in Enshi, Central China. Environmental Pollution, 273, 116507. doi: 10.1016/j.envpol.2021.116507.

Ma SM, Zhu LX, Wang ZF, Liu CM, Hu SQ. 2006. The distribution patterns of rare earth elements (REE) in soil and their tracing role in alluvial plain. Geophysical and Geochemical Exploration, 30(2), 100–103 (in Chinese with English abstract).

McLennan SM. 1993. Weathering and Global Denudation. The Journal of Geology, 101(2), 295–303. doi: 10.1086/648222.

Michele LWT, Juli WF, John GE, Richard IG, Lisa L. 2014. Contaminants from cretaceous black shale: II. Effect of geology, weathering, climate, and land use on salinity and selenium cycling, Mancos Shale landscapes, southwestern United States. Applied Geochemistry, 46, 72–84. doi: 10.1016/j.apgeochem.2013.12.011.

Muller J, Abdelouas A, Ribet S, Grambow B. 2012. Sorption of selenite in a multi-component system using the “dialysis membrane” method. Applied Geochemistry, 27(12), 2524–2532. doi: 10.1016/j.apgeochem.2012.07.023.

Natasha, Muhammad S, Nabeel KN, Sana K, Behzad M, Irshad B, Muhammad IR. 2018. A critical review of selenium biogeochemical behavior in soil-plant system with an inference to human health. Environmental Pollution, 234, 915–934. doi: 10.1016/j.envpol.2017.12.019.

Nesbitt HW, Young GM. 1982. Early Proterozoic climates and plate motions inferred from major element chemistry of lutites. Nature, 299, 715–717. doi: 10.1038/299715a0.

Newman R, Waterland N, Moon Y, Tou JC. 2019. Selenium biofortification of agricultural crops and effects on plant nutrients and bioactive compounds important for human health and disease prevention-A review. Plant Foods for Human Nutrition, 74(4), 449–460. doi: 10.1007/s11130-019-00769-z.

Ni RX, Luo KL, Tian XL, Yan SG, Zhong JT, Liu MQ. 2016. Distribution and geological sources of selenium in environmental materials in Taoyuan County, Hunan Province, China. Environmental Geochemistry and Health, 3(3), 927–938. doi: 10.1007/s10653-015-9772-2.

Ran Y, Liu Z. 1994. The content and distribution of rare earth elements in the main soils of China. Journal of the Chinese Society of Rare Earths, 12(3), 248–252 (in Chinese).

Ren R, Chao X, Zhang LJ, Zhi Q, Xu CL, Ling DD, Ma YM, Chen JP, Qiao XX, Du SX. 2024. Establishment and application of evaluation system for development and utilization of selenium-rich land —A case study in Lintong District, Xi’an. Geology in China, 51(2), 676–688 (in Chinese with English abstract). doi: 10.12029/gc20230813003.

Reynolds RJB, Jones RR, Heiner J, Crane KM, Pilon-Smits EAH. 2020. Effects of selenium hyperaccumulators on soil selenium distribution and vegetation properties. American Journal of Botany, 107(7), 970–982. doi: 10.1002/ajb2.1500.

Shi ZM, Pan PJ, Feng YW, Kan ZZ, Li ZH, Wei F. 2017. Environmental water chemistry and possible correlation with Kaschin-Beck Disease (KBD) in northwestern Sichuan, China. Environment International, 99, 282–292. doi: 10.1016/j.envint.2016.12.006.

Sun GX, Meharg AA, Li HF, Chen Z, Yang L, Chen SC, Zhu YG. 2016. Distribution of soil selenium in China is potentially controlled by deposition and volatilization? Scientific Reports, 6(1), 20953. doi: 10.1038/srep20953.

Tan JA. 1989. The Atlas of Endemic Diseases and Their Environments in the People’s Republic of China. Beijing, Science Press, 39–39 (in Chinese).

Tan JA, Zhu WY, Wang WY, Li RB, Hou SF, Wang DC, Yang LS. 2002. Se in soil and endemic diseases in China. Science of the Total Environment, 284, 227–235. doi: 10.1016/S0048-9697(01)00889-0.

Thomson CD. 2004. Assessment of requirements for Se and adequacy of Se status: A review. European Journal of Clinical Nutrition, 58(3), 391–402. doi: 10.1038/sj.ejcn.1601800.

Wang HY, Zeng DM, Guo ZJ, Cheng XM, Peng M, Sun Y. 2021. Selenium threshold for the delimitation of natural selenium-enriched land. Environmental Science, 42(1), 333–342 (in Chinese with English abstract). doi: 10.13227/j.hjkx.202005148.

Wang QY, Zhang JB, Zhao BZ, Xin XL, Deng XH, Zhang HL. 2016. Influence of long-term fertilization on selenium accumulation in soil and uptake by crops. Pedosphere, 26(1), 120–129. doi: 10.1016/S1002-0160(15)60028-5.

Wang RQ, Zhang ZM, Chao X, Feng HY, Yang ZF. 2022. A study of the Selenium speciation in paddy soil and status of selenium enriched rice in western part of Ankang City, Shaanxi Province. Geology in

China, 49(2), 398–408 (in Chinese with English abstract). doi: 10.12029/gc20220204.

Wang XK, Huang ZF, Su MX, Li SB, Wang Z, Zhao SZ, Zhang Q. 2007. Characteristics of reference and background values of soils in Hetao Area. Rock and Mineral Analysis, 26(4), 287–292 (in Chinese with English abstract). doi: 10.15898/j.cnki.11-2131/td.2007.04.012.

Wang XQ, Liu QQ, Liu HL, Hu QH, Wu H, Wang W. 2021. Key elements and human health: Is China's arable land selenium-deficient? Earth Science Frontiers, 28(3), 412–423 (in Chinese with English abstract). doi:10.13745/j.esf.sf.2021.1.13.

Wang ZJ, Gao YX. 2001. Biogeochemical cycling of selenium in Chinese environments. Applied Geochemistry, 16(11), 1345–1351. doi: 10.1016/S0883-2927(01)00046-4.

Wang ZW, Liu YM, Wang ZL, Miao YT. 2022. Distribution and environmental significance of rare earth elements typical protected vegetable soil, Northern China. Environmental Science, 43(4), 2071–2080 (in Chinese with English abstract). doi: 10.13227/j.hjkx.202108030.

Wei H, Wei XF, Wang JB, Zhu SJ, Yang F, Liang Z, Tian XX, Li W, Jia WR, Yu KN. 2024. Geochemical characteristics, geological genesis and ecological environment evaluation of soil selenium in Chengde, Hebei Province. Geology in China, 51(4), 1290–1303 (in Chinese with English abstract). doi: 10.12029/gc20211017001.

Wu J. 2018. The distribution of soil selenium in Shouning County of Fujian Province and its influencing factors. Geology in China, 45(6), 1167–1176 (in Chinese with English abstract). doi: 10.12029/gc20180607.

Xia W, Yang J, Xiang JQ, Yang LZ, Wang F, Wang WW, Li CC, Huang B, Xu CY, Zhao M. 2023. Source analysis and bioenrichment of selenium-rich soil in the Jianghan plain: A case study from the northeast of Shayang County. Acta Geologica Sinica, 97(5), 1670–1682 (in Chinese with English abstract). doi: 10.19762/j.cnki.dizhixuebao.2022033.

Xiao KC, Tang JJ, Chen H, Li DJ, Liu YX. 2020. Impact of land use/land cover change on the topsoil selenium concentration and its potential bioavailability in a karst area of southwest China. Science of the Total Environment, 708, 135201. doi: 10.1016/j.scitotenv.2019.135201.

Xu XS, Luo JL, Huang FQ, Wang HH, Xia XQ, Lu J, Zhang ZH, Zhu LF. 2022. Construction of the evaluation system for Se-rich arable land and its application in Xinxu Town, Xintian County, Hunan Province. Geology in China, 49(3), 789–801 (in Chinese with English abstract). doi: 10.12029/gc20220308.

Xu YF, Hao Z, Li YH, Li HR, Wang L, Zang ZF, Liao XY, Zhang R. 2020. Distribution of selenium and zinc in soil-crop system and their relationship with environmental factors. Chemosphere, 242, 125289. doi: 10.1016/j.chemosphere.2019.125289.

Yang GQ, Wang SZ, Zhou RH, Sun SZ. 1983. Endemic Se intoxication of humans in China. American Journal of Clinical Nutrition, 37(5), 872–881. doi: 10.1093/ajcn/37.5.872.

Yang SY, Li CX. 1999. Research progress in REE tracerfor sediment source. Advances in Earth Science, 14(2), 164 (in Chinese with English abstract).

Yang ZF, Yu T, Hou QY, Yang Y, Fu YR, Zhao XL. 2012. Geochemical characteristics of soil selenium in farmland of Hainan Island. Geoscience, 26(5), 837–849 (in Chinese with English abstract).

Yu C, Wu LJ, Zhang YL, Wang XY, Wang ZC, Zhang Z. 2022. Effect of groundwater on the ecological water environment of typical inland lakes in the Inner Mongolian Plateau. Journal of Groundwater Science and Engineering, 10(4), 353–366. doi: 10.19637/j.cnki.2305-7068.2022.04.004.

Yu T, Yang ZF, Wang R, Zeng QL, Hou WL. 2018. Characteristics and sources of soil selenium and other elements in typical high selenium soil area of Enshi. Soils, 50(6), 1119–1125 (in Chinese with English abstract). doi: 10.13758/j.cnki.tr.2018.06.009.

Zhou F, Peng Q, Wang M, Xue MY, Zhai H, Liu NN, Wang MK, Qi MX, Liang DL. 2022. Advances in the evaluation of selenium bioavailability in soil-plant system. Chinese Science Bulletin, 67(6), 461–472 (in Chinese with English abstract). doi: 10.1360/TB-2020-1268.

Zhou GH. 2020. Research progress of selenium-enriched land resources and evaluation methods. Rock and Mineral Analysis, 39(3), 319–336 (in Chinese with English abstract). doi: 10.15898/j.cnki.11-2131/td.201911140158.

Zhu LX, Ma SM, Zhou GH, Zheng LG. 2002. Characters of soil elements and its tracing application in alluvial plain. Geology and Exploration, 38(4), 56–59 (in Chinese with English abstract).